# Phantom generation for Neural Networks

Alejandro Sanz-Sanchez ,[1] Francisco Brandan García-Aparisi, Pablo Mesas-Lafarga, Joan Prats-Climent, María José Rodríguez-Álvarez

Instituto de Instrumentación Para Imagen Molecular (I3M),Universitat Politècnica de València (UPV) Camí de Vera s/n, València, Spain.

## 1 Introduction

Positron emission tomography (PET) is a functional medical imaging technique that allows the extraction of information from biological processes (or functional), such as blood flow or metabolism. To be able to do this, a radiotracer is injected into the patients body, usually fluorodeoxyglucose-18 (FDG) that is a glucose analog with the radionuclide fluorine-18 that naturally emits positrons. This type of medical image technique is widely used in oncology as usually cancerous cells or tumors uptakes high quantities of glucose and thus are easily detected as a region with elevated activity by the PET scanner.

Positron emission tomography (PET) data acquisition is based on the detection of two 511 KeV annihilation photons that originate from the use of FDG positron emission. Usually prior to the first clinical use of a scanner it must be calibrated using an imaging phantom (or just phantom) that it is a device that simulates an standardized body and is used to evaluate, analyze and tune the detector.

The obtained data from a PET scan has to be reconstructed, there exist a multitude of reconstruction algorithms, traditionally reconstructions were performed using non-iterative methods such as the Inverse Radon Transform, Filtered Back Projection (FBP) and in more recent years, there was a shift into iterative reconstruction algorithms such as in Maximum Likelihood Expectation Maximization (MLEM) or Ordered Subset Expectation Maximization (OSEM) that reconstruct the data into a 3D image space that represents the real physical object that has been detected by the system.

There has been advancements in the field of Artificial Intelligence (AI) with the development of artificial neural networks that have enabled multiple uses in a wide range of industries. The use of AI systems has also been adopted in medical imaging, therefore in PET imaging reconstruction state of the art there has been an adoption of Convolutional Neural Networks (CNNs) in order to perform the reconstruction from data obtained by the scanner as input for the Neural Network and to obtain the reconstructed image [1],[2] One of the main drawbacks of the use of Neural Networks is that they require a large amount of images in order to train the neural network so it can reconstruct the data to the real image space.

To address this problem, it is our intent to generate programmatically different types of medical phantom images that will be later used to train a neural network reconstructor of PET images. In our case as the phantoms will be generated via programming and to validate our results we will simulate the data acquisition step using a Monte Carlo simulation software called GATE.[4]

[1] alsan23a@i3m.upv.es

# 2 Methods

To generate the synthetic phantoms a pipeline was developed using Python[5] that allowed the tuning of several parameters of the geometries of different phantoms, in order to generate likewise phantoms, that were similar to the standardized ones used in the scanners calibration.

In the following table it is shown some of the most widely used phantoms in PET imaging:

| Phantom name | Main geometry | Secondary geometry | Number of secondary geometries |
|---|---|---|---|
| NEMA | Cylinder | Cylinder | 6 |
| Jaszczak | Cylinder | Sphere | 6 |
| Derenzo | Cylinder | Cylinder | 116 |
| Shepp-Logan | Ellipse | Ellipse | 10 |

Table 1: Types of phantoms and geometries

In figure 1 can be seen some samples of the mentioned phantoms:

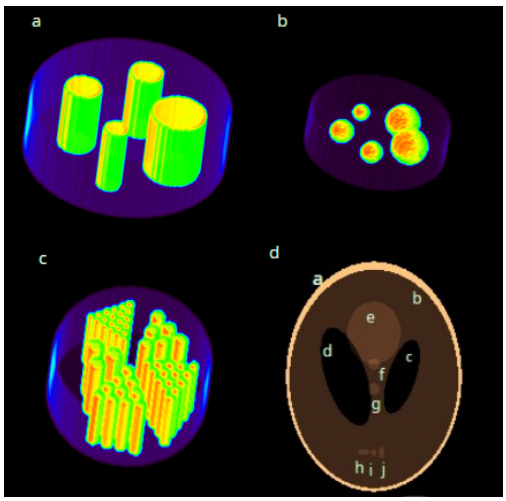


Figure 1: Phantoms: a) NEMA , b) Jaszczak, c) Derenzo , d) Shepp-Logan

Considering the differences of each phantom the goal was to generate 3D voxelized phantoms, modifying the original shapes, sizes and positions of the secondary geometries within each generated phantom. In the next subsections will explain the particularities and processes implemented to generate these phantoms.

## 2.1 Nema-like phantom

A standard Nema NU 4 [6] phantom is made up of a main geometry that is cylinder that contains as a secondary geometry 6 smaller cylinders in a radial disposition from the center of the phantom of different sizes. This phantom is used for the image quality assessment in small animal imaging PET scanners and it is widely used to compare the differences between PET systems. Some of the parameters that can be evaluated are count rate performance, scatter fraction, sensitivity and spatial resolution.

In order to generate this type of phantom the following parameters will be considered:

| Phantom name | Main geometry | Parameter | Tuneable | Range | Secondary geometry | Parameter | Tuneable | Range |
|---|---|---|---|---|---|---|---|---|
| NEMA | Cylinder | Radius (mm) | Yes | 30 - 60 | Cylinder | Radius (mm) | Yes | Depends on number of geometries |
| | | Heigth (mm) | Yes | 20 - 50 | | Heigth (mm) | No | |
| | | | | | | Number | Yes | 3 - 8 |

Table 2: Nema parameters

In the standard Nema phantom, the secondary cylinders inserted into the main cylinder have to be equidistant. As a consequence of this, in order to develop a NEMA-like phantom in which the number of secondary cylinders is modified, it will be needed to split the main cylinder into sectors and then in order to avoid overlapping of the secondary cylinders, calculate the maximum radius that could fit in a circular sector, as the radius of the secondary cylinders also will be tunable.

The procedure to generate a NEMA-like phantom was:

- Select randomly the tunable parameters of the main cylinder and the number of secondary cylinders.
- Considering the number of secondary cylinders split the main cylinder in sectors and calculate the maximum radius in a circular sector.
- Select randomly the tunable parameters of the secondary cylinders.
- Generate an empty array with the dimensions of the phantom image to generate
- Iterate through the array considering the voxelized coordinates of the main cylinder and secondary cylinders to assign an activity value, being the higher activity values in the secondary cylinders.

## 2.2 Jaszczak-like phantom

The jaszczak phantom is made up of a main geometry of a cylinder and the secondary geometries of 6 spheres in the same disposition as the NEMA phantoms. This phantom is generally used for the evaluation of the spatial resolution, sensitivity, image uniformity and attenuation correction accuracy.
The parameters that will be tuned during the generation are:

| Phantom name | Main geometry | Parameter | Tuneable | Range | Secondary geometry | Parameter | Tuneable | Range |
|---|---|---|---|---|---|---|---|---|
| Jaszczak | Cylinder | Radius (mm) | Yes | 30 - 60 | Sphere | Radius (mm) | Yes | Depends on number of geometries |
| | | Heigth (mm) | Yes | 20 - 50 | | Heigth (mm) | No | |
| | | | | | | Number | Yes | 3 - 8 |

Table 3: Jaszczak parameters

The procedure to generate a Jaszczak-like phantom was:

- Select randomly the tunable parameters of the main cylinder and the number of secondary spheres.

- Considering the number of secondary spheres split the main cylinder in sectors and calculate the maximum radius in a circular sector.
- Select randomly the tunable parameters of the spheres.
- Generate an empty array with the dimensions of the phantom image to generate
- Iterate through the array considering the voxelized coordinates of the main cylinder and secondary spheres to assign an activity value, being the higher activity values in the spheres.

### 2.3 Derenzo-like phantom

The Derenzo phantom is made up of a main geometry being a cylinder and the secondary geometries being a series of smaller cylinders. The main difference with the NEMA-like phantom is that the secondary geometries, instead of being single cylinders, these are a series of cylinders arranged according to a figurate number being based on the triangular number. As such each sector of the main geometry will contain an increasing the number of secondary cylinders accordingly to the progression of the triangular numbers. Following the formula:

$$T_n \equiv \sum_{k=1}^{n} = \frac{1}{2}n(n+1) = \binom{n+1}{k} \tag{1}$$

Being $\binom{n}{k}$ a binomial coefficient.

This phantom is used for the evaluation of the imaging system resolution by measuring the full width half maximum (FWHM) between the secondary cylinders, as the series of smaller cylinders within each sector always have the same radius and are equally distanced between them. The parameters that will be tuned during the generation are:

| Phantom name | Main geometry | Parameter | Tuneable | Range | Secondary geometry | Parameter | Tuneable | Range |
|---|---|---|---|---|---|---|---|---|
| Derenzo | Cylinder | Radius (mm) | Yes | 40 - 60 | Cylinder | Radius (mm) | Yes | Depends on number of geometries |
| | | Heigth (mm) | Yes | 20 - 50 | | Heigth (mm) | No | |
| | | | | | | Number | Yes | 3 - 7 |

Table 4: Derenzo parameters

The procedure to generate a Derenzo-like phantom was:

- Select randomly the tunable parameters of the main cylinder and the number sectors to split the main cylinder.
- Considering the number of sectors and following the triangular number calculate the number of cylinders that each sector will contain.
- Select the radius of each cylinder, considering the number of cylinder to fit in each sector.
- Generate an empty array with the dimensions of the phantom image to generate
- Iterate through the array considering the voxelized coordinates of the main cylinder and secondary spheres to assign an activity value, being the higher activity values in the spheres.

### 2.4 Shepp-Logan-like phantom

The Shepp-Logan phantom is a mathematically defined phantom that is made up of a main geometry being an ellipse and the secondary geometries another set of ellipses. It resembles the anatomical structures of the human torso, considering organs such as the lungs, heart or liver. This kind of phantoms are used to characterize the detector spatial resolution, noise characteristics, artifact generation or contrast resolution.

The parameters that will be tuned during the generation are:

| Phantom name | Main geometry | Parameter | Tunable | Secondary geometry | Parameter | Tunable |
|---|---|---|---|---|---|---|
| Shepp-Logan | Ellipse | Major Axis | Yes | Ellipse | Major Axis | Yes |
| | | Minor Axis | Yes | | Minor Axis | Yes |
| | | | | | Number | Yes |

Table 5: Shepp-Logan parameters

In this instance the ranges had not being included as a major and minor axis of the phantom are selected at random, with the condition that it does not exceed the dimensions of the voxelized image.
The procedure to generate a Shepp-Logan-like phantom was:

- A range of the major and minor axis values is generated for each ellipse, considering to avoid overlapping between the different secondary ellipses
- Calculate the voxelized coordinates of each ellipse.
- Generate an empty array with the dimensions of the phantom image to generate.
- Iterate through the array considering the voxelized coordinates of the main ellipse and secondary ellipses to assign an activity value, being the higher activity values in the spheres.

### 2.5 Validation of the synthetically generated phantoms

Once the different phantoms generators were developed the subsequent pipeline was developed to check the proper functioning of the generator of phantoms.

- Generate several voxelized phantoms, tuning the parameters in each type of phantom within the set ranges for each phantom.
- Simulate a PET acquisition using a Monte Carlo simulation software.
- Using the MLEM iterative reconstruction algorithm, reconstruct the images from the acquired data.
- Visually compare the images of the voxelized phantoms against the reconstructions.

## 3 Results

In the figure 2 can be seen some examples of the generated phantoms, in all the cases can be seen for each type of phantom that quantitatively the images from the left are the same that the ones on the right. In all the generated voxelized images can be observed that the regions marked as yellow, that correspond to the regions of high activity, are also correctly reconstructed after the

PET acquisition simulation as both images are similar and validates our results.

The phantoms were simulated using the UPV Rigel cluster, as the Monte Carlo simulations are computationally expensive and it required vast CPU computation time in order to validate the results. The simulation of the phantoms shown in the figure 2 required approximately 1700 hours, the data processing took 5 hours and the reconstruction 3.5 hours, for all phantoms.

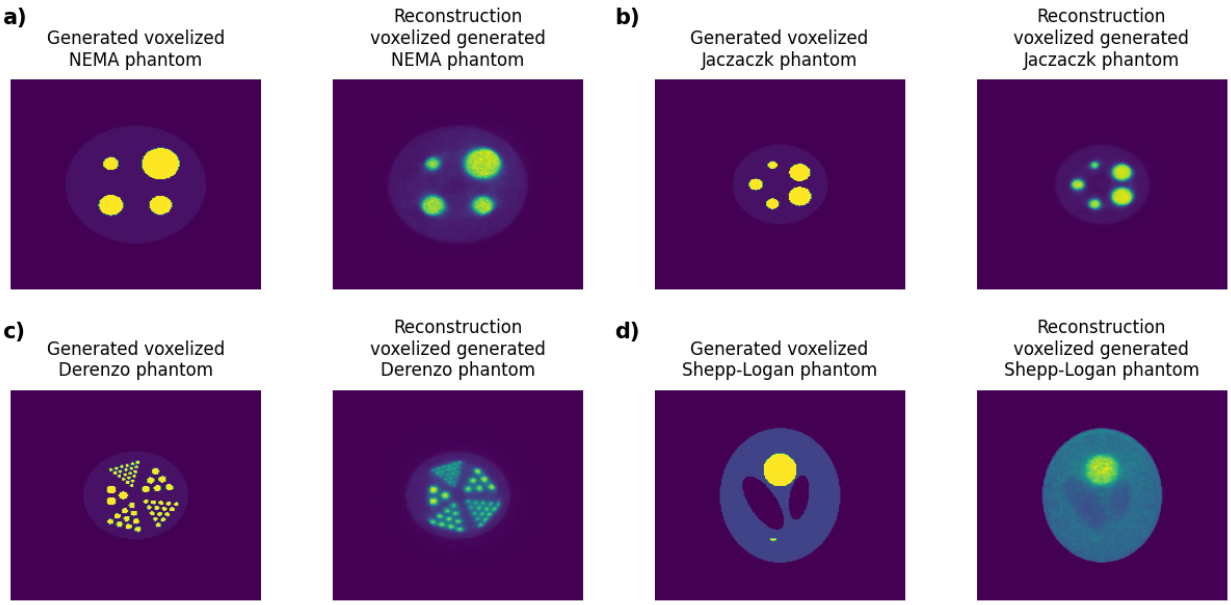


Figure 2: Phantoms: a) NEMA-like voxelized and reconstruction, b) NEMA-like voxelized and reconstruction, c) NEMA-like voxelized and reconstruction, d) NEMA-like voxelized and reconstruction

## 4 Conclusions

As a conclusion it has been proved that implemented phantom generator pipeline works well when in comes to the systematically generation of synthetic phantoms and enables the creation of an indefinite number of phantoms that could be used to generate the necessary images to train a convolutional neural network geared towards the reconstruction of PET imaging reconstruction. As the generated voxelized images and the reconstruction from the simulation results in images that represent the same phantom and these have similar geometries and characteristics as the standardized phantoms used for the calibration of PET scanners.

## Acknowledgements

Thanks to the UPV for the access to the RIGEL Supercomputing cluster of the UPV. I3M MIRG group has access to RIGEL, the supercomputing cluster of the UPV. RIGEL is equipped with 72 CPU parallel processing nodes (BX920S3 nodes, Bull R424E4 nodes and Dell Power Edge R640 nodes). Each node contains 2 Intel Xeon E5-2450 8c/16T processors and 64 GB/RAM DDR3 and 2 dedicated GPU computing nodes (Nvidia Tesla M2075). In 2015 an additional 56 CPU parallel processing nodes (Bull R424E4) were added. 48 nodes contains 2 Intel Xeon E5-2630v3 8c/16T processors and 64 GB/RAM DDR4 and 8 nodes with Intel Xeon E5-2680v3 12c/24T and 128 GB/RAM DDR4. Thanks to the European Union and the Valencian Comunity with the FEDER funds 2014-2020 an additional 27 CPU parallel processing nodes were added. Each node contains 2 Xeon Gold 6154 18c/36T with 24 nodes of 192 GB/RAM DDR4 and 5 nodes of 768 GB/RAM DDR4. It also includes a high-speed interconnection network and a RAID storage system that provides unified disk space to users. Access to this cluster, together with the Institute's own huge infrastructure, makes its management and maintenance critical. Also, during 2022, an expansion of RIGEL the scientific cluster, valued at 1.5000.000 €will be acquired (with the support of Spanish Research State Agency and the European Union with Next Generation Funds, ref: EQC2021-007509-P).

## References

[1] Xie Z, Li T, Zhang X, Qi W, Asma E, Qi J. Anatomically aided PET image reconstruction using deep neural networks. Med Phys. 2021 Sep;48(9):5244-5258. doi: 10.1002/mp.15051. Epub 2021 Jul 28. PMID: 34129690; PMCID: PMC8510002.

[2] Häggström I, Schmidtlein CR, Campanella G, Fuchs TJ. DeepPET: A deep encoder-decoder network for directly solving the PET image reconstruction inverse problem. Med Image Anal. 2019 May;54:253-262. doi: 10.1016/j.media.2019.03.013. Epub 2019 Mar 30. PMID: 30954852; PMCID: PMC6537887.

[3] Merlin T, Stute S, Benoit D, Bert J, Carlier T, Comtat C, Filipovic M, Lamare F, Visvikis D. CASToR: a generic data organization and processing code framework for multi-modal and multi-dimensional tomographic reconstruction. Phys Med Biol. 2018 Sep 10;63(18):185005. doi: 10.1088/1361-6560/aadac1. PMID: 30113313.

[4] Sarrut D, Arbor N, Baudier T, Borys D, Etxebeste A, Fuchs H, Gajewski J, Grevillot L, Jan S, Kagadis GC, Kang HG, Kirov A, Kochebina O, Krzemien W, Lomax A, Papadimitroulas P, Pommranz C, Roncali E, Rucinski A, Winterhalter C, Maigne L. The OpenGATE ecosystem for Monte Carlo simulation in medical physics. Phys Med Biol. 2022 Sep 8;67(18). doi: 10.1088/1361-6560/ac8c83. PMID: 36001985.

[5] Van Rossum, Guido and Drake, Fred L., Python 3 Reference Manual. Scotts Valley, CA, CreateSpace, 2009.

[6] https://www.nema.org/standards/view/Performance-Measurements-of-Small-Animal-Positron-Emission-Tomographs